Applied Nanoscience (2023) 13:7455–7468
https://doi.org/10.1007/s13204-023-02926-y

ORIGINAL ARTICLE

Extraction, properties and use of nanocellulose from corn crop residues

V. A. Barbash[1] · O. V. Yashchenko[1] · O. S. Yakymenko[1] · V. D. Myshak[2]

Received: 16 December 2022 / Accepted: 4 July 2023 / Published online: 20 July 2023

Abstract

The study describes the extraction of cellulose and nanocellulose (NC) from corn crop residues (CCR), the world's largest cereal crop. The effect of mechanical sieving and washing of CCR in cold and hot water on the content of chemical elements in their ash was investigated. It is recommended to sift crushed CCR from sand and dust before thermochemical treatment. Corn organosolv cellulose (OCC) was obtained by an environmentally friendly method using a solution of peracetic acid. SEM data confirmed the destruction and decrease in the size of CCR fibers during their thermochemical treatments. FTIR and XRD data showed that the influence of chemicals and temperature leads to a decrease in the content of residual lignin, the lateral order index, the apparent size of crystallites, and an increase in the crystallinity index in corn cellulosic materials in the following order: CCR—corn pulp after alkaline extraction—OCC—NC. DLS, AFM, and TEM data confirmed that NC particles had a transverse size in the range of 5–65 nm and a length of up to several micrometers. The positive effect of the use of corn NC on the improvement of cardboard indicators and the reduction of the consumption of harmful chemical auxiliary substances is shown. Corn NC with a density of up to 1.2 g/cm^3, a tensile strength of up to 43 MPa, and a crystalline index of 74.9% can of composite materials and as a basis for obtaining smart electronic devices.

Keywords Corn crop residues · Organosolv cellulose · Hydrolysis · Nanocellulose · Property · Cardboard

Introduction

The implementation of the doctrine of reducing the use of exhaustible sources of energy is aimed at improving the state of the environment and achieving the goal set by the Paris Agreements aimed at "zero" carbon emissions by 2050 (Ilari et al. 2022). Therefore, in recent years, new sources of raw materials and the development of new materials to replace polymers from fossil sources—oil, gas, and coal—have been intensively researched. These types of raw materials include cellulosic sources, in particular wood and agricultural waste. Cellulose is the most abundant natural renewable biodegradable material on earth (Tu et al. 2020). Cellulose macromolecules have the characteristics of high hydrophilicity and density of hydroxyl groups, which contributes to the modification of functional groups with the formation of new products with unique properties (Liu et al. 2022; Nagarajan et al. 2021). Cellulosic sources are environmentally safer and affordable raw materials for the extraction of nanocellulose. Nanocellulose (NC) is one of the most promising substances from cellulose-containing raw materials due to its unique properties—excellent mechanical properties relative to its weight and very high elastic modulus, a large specific surface area, and high length-to-diameter ratio (Sun et al. 2016), high transparency and chemical resistance, low coefficient of thermal expansion (Lee et al. 2014) and non-toxic character. Exceptional properties of NC depend on the characteristics of the raw materials and methods of obtaining nanocellulose (Deepa et al. 2015). NC is traditionally classified into cellulose nanofibers (CNF), cellulose nanocrystals (CNC), and bacterial nanocellulose (Azeredo et al. 2017; Sihag et al. 2022). NC is widely used in industry to increase the mechanical strength and improve the barrier properties of paper and cardboard (Reshmy et al. 2020), polymer and cement composites (Isogai 2020), electric batteries (Kang et al. 2020) and in the field of water treatment (Gopakumar et al. 2018), medical (Alavi 2019) and biomedical applications (Du et al.

✉ V. A. Barbash
v.barbash@kpi.ua

[1] National Technical University of Ukraine "Igor Sikorsky Kyiv Polytechnic Institute", Kiev, Ukraine

[2] Institute of Macromolecular Chemistry of the National Academy of Sciences of Ukraine, Kiev, Ukraine

2019), food packaging and green nanocomposite materials (Abdul Khalil et al. 2014). NC can be extracted from many renewable natural sources of cellulose and is therefore considered a cost-effective substitute for synthetic fibers such as carbon and glass (Randhawa et al. 2022).

Different methods are used for the extraction of NC from cellulose-containing raw materials. These include mechanical treatments such as high-pressure homogenization (Ren et al. 2014), high-intensity ultrasonication (Hu et al. 2017), cryocrushing (Kaur et al. 2017), microfluidization (Nehra and Chauhan 2021), grinding (Jiang et al. 2019) with or without enzymatic and chemical pretreatment. Mechanical treatments are characterized by significant energy consumption (Kumar et al. 2020) and lead, as a rule, to obtain CNF. Energy consumption can be reduced by carrying out preliminary enzymatic treatment, which is characterized by high cost and labor intensity, or chemical processing of cellulosic sources (Sharma et al. 2019). Chemical methods of nanocellulose extraction use mineral and organic acids (Benchikh and Merzouki 2019; Biana et al. 2018), oxidants: 2,2,6,6-tetramethylpiperidine-1-oxyl (Madivoli et al. 2020) and phthalimide-N -oxyl (Coseri 2009), deep eutectic solvents (Su et al. 2021). Acid hydrolysis of cellulose is considered to be the most effective method of removing amorphous and disordered areas of cellulose, which provides a high degree of crystallinity of NC. The use of chemical methods leads to the formation of CNC, which usually has a smaller transverse size than CNF (Isogai 2020).

To extraction NC, bleached wood pulp with a small residual content of lignin and extractive substances is often used as a starting material. For the production of bleached wood pulp in the global pulp industry, the dominant production technologies are sulfate and sulfite methods, which pollute the air and water bodies with harmful toxic sulfur compounds (Smook 2003). Organic compounds make it possible to replace sulfur-containing solutions for the preparation of cooking solutions and reduce harmful emissions into the atmosphere. For example, acetic acid and peracetic acid, due to their relatively low cost, are considered potential agents to achieve significant delignification of cellulosic sources (Hu et al. 2022). Peracetic acid is formed from a mixture of acetic acid and hydrogen peroxide and is characterized by excellent delignification and bleaching properties with minimal pulp damage (Karbalaei et al. 2019). The peracetic acid pulping process is applied to both woody and non-woody plant materials and is carried out at a low temperature, which contributes to low energy consumption (Deykun et al. 2018).

An alternative source of cellulose to wood is non-wood plant materials, the use of which will contribute to the preservation of wood stocks and the improvement of the environment. The first place in the world among grain crops in terms of annual volume of fibrous mass (750 million tons) is occupied by corn stalks (Fahmy et al. 2017). It is used as a valuable raw material for the production of bioethanol and solid biofuel, animal feed, and raw material for the production of pulp and cardboard-paper products (Smith et al. 2004). After harvesting corn for grain, a large amount of corn crop residues (CCR) remains, which is considered a source of fibers for the production of cellulose and nanocellulose. There are no data on the production of cellulose from CCR by environmentally safe methods and the extraction of nanocellulose from it. Therefore, the purpose of this work is to obtain cellulose from corn crop residues by an ecologically friendly method and to extract nanocellulose from it by acid hydrolysis with the determination of its characteristics and to investigate the possibility of using corn NC in the production of one of the mass types of the paper industry—cardboard for flat layers of corrugated cardboard.

Experimental section

Materials and chemicals

The corn crop residues (CCR) were collected from the Sumy region of Ukraine after the 2021 harvest. The collected samples of CCR were crushed on a disintegrator and sieved on sieves with holes of 0.25 mm and 0.5 mm to separate the fibrous part of the CCR from leaves, dust and small parts of raw materials. The raw materials of these three fractions were stored in desiccators to maintain constant humidity. The fraction of CCR remaining on the sieve with holes of 0.5 mm was used to obtain cellulose. For comparison, the sieved raw materials were pre-washed with cold or hot water before cooking the pulp.

Chemicals: sodium hydroxide, glacial acetic acid, hydrogen peroxide, sulfuric acid and ethanol were analytical grade or chemically pure. They were used to obtain corn cellulose and nanocellulose and determine the content of the main chemical components according to TAPPI standards (TAPPI 2004). Chemical analyses were carried out for the different components, namely: T-257 for hot-water soluble substances, T-212 for soluble in 1% NaOH solution, T-204 for ethanol–benzene extractables, T-222 for lignin, T-211 for ash and cellulose by the Kűrschner-Hoffer method.

Obtaining of the organosolv corn cellulose

The general scheme for obtaining organosolv corn cellulose (OCC) and nanocellulose from CCR is shown in Fig. 1. Briefly, the preparation of OCC involved three stages of CRC processing. In the first stage, the CCR was treated with a 5% NaOH solution at a liquid-to-solid ratio of 10:1 at a temperature of 98 ± 2 °C for 180 min. As a result of filtering the spent solution and washing the fibrous mass

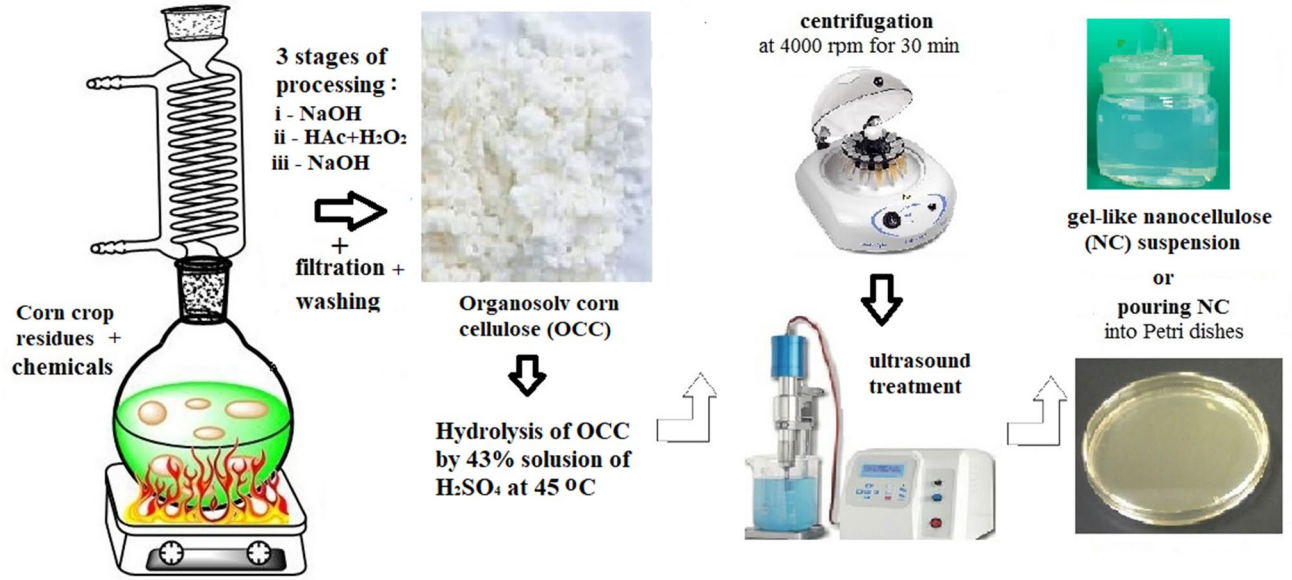

Fig. 1 The scheme of extraction of OCC and corn NC from CCR

with distilled water and squeezing it, corn pulp after alkaline extraction (CPA) was obtained. In the second stage, to remove residual lignin and extractives, organosolv cooking was carried out using a solution of glacial acetic acid and 35% hydrogen peroxide in a volume ratio of 7:3 with a liquid-to-solid ratio of 10:1 at a temperature of 97 ± 2 °C for 30–180 min. In the third stage, to reduce the residual content of lignin and mineral substances in the pulp, additional alkaline treatment was carried out with sodium hydroxide solution with a concentration of 5% for 30 min at a temperature of 98 ± 2 °C. After filtering and washing several times with distilled water and squeezing, OCC was obtained. The OCC was stored in a wet state in a sealed bag for the extraction of nanocellulose from it. Never dried cellulose is better, as dried samples irreversibly lose access to the surface during the drying process. Using never-dried OCC does not require the consumption of energy for drying and grinding since dried cellulose fibers lose the ability to swell and percolate due to irreversible cornification (Barbash et al. 2022).

Extraction of the corn nanocellulose

The preparation procedure of corn nanocellulose was brief as follows. 1 g of the OCC was placed in a heat-resistant glass, into which 10 ml of a 43% solution of sulfuric acid was poured drop by drop, and then it was placed in a thermostat with a temperature of 60 °C for 60 min and periodically stirred with a glass rod. The hydrolysis was stopped by tenfold dilution with distilled water and subsequent cooling of the suspension to room temperature. The hydrolyzed nanocellulose was washed several times with distilled water to remove all non-reacted reagents and free ions by centrifugation at 4000×*rpm* until neutral pH was reached. To improve the texture of NC, its suspension was treated with ultrasound for one hour using an ultrasonic disintegrator UZDN-A (SELMI, Ukraine) with a frequency of 22 kHz. The resulting transparent gel-like corn NC suspension with a concentration of about 1% was poured into Petri dishes and dried at room temperature to obtain films that were analyzed or stored at room temperature in airtight containers for use in cardboard compositions.

Preparation of handsheets

Standard laboratory handsheet samples of cardboard for flat layers of corrugated cardboard were prepared using a Rapid-Kothen machine according to TAPPI T205 sp-02. The handsheets of 175 ± 10 g/m^2 were produced from waste paper. The waste paper was beaten in a Valley beater to 45°SR (Shopper-Rigler). The consumption of alkyl ketene dimer (AKD) was 1.5% or 3.0 kg/t and the consumption of corn NC was 1.5, 3.0, 5.0, and 10.0 kg/t of cardboard. These sheets were conditioned in a chamber at 23 °C and 50% humidity for 24 h before determining their physical and mechanical parameters and compared with the requirements of the standard.

Research methods

The morphological structure of the CCR, CPA, OCC, and NC films was analyzed by *scanning electron microscopy* (*SEM*). The research was carried out on a PEM-106I

microscope (SELMI, Ukraine) at an accelerating voltage of 20 kV. Before conducting the study, a layer of gold coating was applied to the sample using an "ion sputter". *X-ray fluorescence analysis* of mineral residues of the CCR was carried out on the express chemical composition analyzer "EXPERT 3L" (Ukraine). The *particle size* distribution of nanocellulose in aqueous suspensions was determined by the method of *dynamic light scattering* (*DLS*) using a particle size analyzer "Zetasizer Nano" (Malvern Instruments Ltd, UK), operating in the range of 0.3 nm–10 µm. 3 parallel experiments were conducted in disposable plastic cuvettes with a volume of 3 ml of tenfold diluted corn nanocellulose dispersions at a temperature 25 °C.

Fourier transform infrared spectroscopy (*FTIR*) spectra of the CCR, CPA, OCC and corn NC films were recorded on Tensor 37 Fourier-transform infrared spectrometer (BRUKER, Germany) with wave ranges between 300 and 4100 cm^{-1}. Samples for research were mixed with KBr and pressed into tablets. *X-ray diffraction (XRD)* was measured for CCR, CPA, OCC, and NC samples using an Ultima IV diffractometer (Rigaku, Japan) with a Cu Kα radiation source ($\lambda = 0.15418$ nm) operating at 50 kV and 30 mA. The XRD patterns were obtained over the angular range $2\theta = 5°–70°$ with a phase of 0.04 and a scan time of 5 min. The *crystallinity index* (*CrI*) of the corn cellulosic materials was calculated from the heights of the peak of the crystalline phase 200 (I_{200}) and the minimum intensity between the peaks 200 and 110, which corresponds to the amorphous phase (I_{am},) using Segal's method (Segal et al. 1959):

$$\mathrm{CrI}\ (\%) = \left[\left(I_{200} - I_{\mathrm{am}}\right)/I_{200}\right] \times 100, \quad (1)$$

where I_{200} is the intensity of the (200) reflection for the crystalline phase at $2\theta = 21.5° \pm 0.7°$ and I_{am} is the intensity of the amorphous phase at $2\theta = 17.8° \pm 1.5°$.

The apparent *crystallite size* (*CrS*) of cellulose I structure in respect of (200) plane was calculated using the Scherrer equation (Torlopov et al. 2017):

$$\mathrm{CrS\ (nm)} = K \times \lambda/(\beta \times \cos\theta), \quad (2)$$

where K is a constant of value 0.94, λ is the X-ray wavelength, $\beta = (B–b)$ or $\beta = (B^2–b^2)^{0.5}$, when B is the observed Full Width at Half Maximum (FWHM), and b is the broadening in the peak due to the instrument in radians, θ denotes the Bragg's angle of the X-ray diffraction peak (200).

The morphological and topographic structure of the surface of the extracted corn NC was determined by *atomic force microscopy* (*AFM*) using the Solver Pro M (NT-MDT) device. The measurement speed using a silicon cantilever in a tapping mode was 0.6 lines/s, and the scanning area was 2×2 µm^2. The morphology of NC was also examined by *transmission electron microscopy* (*TEM*) using a TEM Selmy EMV-125. For this, diluted NC suspensions were applied to a copper grid with a carbon coating 5–10 nm thick and dried in air for 15 min. TEM analysis was performed at room temperature using an accelerating voltage of 75 kV. The *transparency* of corn NC films was determined at a wavelength of 600 nm on a double-beam spectrophotometer 4802 (UNICO, USA) with a resolution of 1 nm.

The thermostability of cellulose-containing corn materials was investigated by *thermogravimetric (TG) and derivative thermogravimetric (DTG)* analyzes using a Q50 thermal analyzer (TA Instrument, USA). Samples of 10 mg were heated from 25 to 600 °C at a heating rate of 10 °C/min in a nitrogen atmosphere with a gas flow rate of 30 ml/min. Weight loss was recorded and processed by a program using computer technology.

The *density* and *tensile strength* of corn NC films were determined according to ISO 534:1988 and ISO 527-1, respectively. To determine the tensile strength, rectangular strips of NC films 10×25 mm were used. The tests were carried out on TIRAtest-2151 instrument equipment (Germany) with a 2 N load at a crosshead speed of 0.5 mm/min. At least five samples of NC films were examined and statistically processed. Stress and strain data were recorded and stored in a data file via a GPIB interface controlled by a homemade protocol programmed in LabView 7.0. *Physico-mechanical properties* of the cardboard were determined in accordance with the following standards: absolute compressive resistance according to ISO 2758 (Tappi T 403); ring crush test (RCT) according to ISO 12192 and water absorption ($Cobb_{60}$) according to ISO 535. These properties were calculated on five test pieces of cardboard for each composition, expressing the results as an average and standard deviation.

Results and discussion

Chemical composition of plant raw materials

As a result of sieving the raw materials of the corn crop residues on sieves with holes with a diameter of 0.5 mm and 0.25 mm, three fractions were obtained: I—a large fraction that remained on a sieve with holes of 0.5 mm (68.5% of the mass of the raw material); II—fraction with particles of 0.5–0.25 mm in size (13.2%), III—fraction of fine raw materials and dust that passed through the sieve with holes with a diameter of 0.25 mm (18.3%). It was determined that fraction I had a lower ash content (3.2%) compared to fractions II and III, 5.4% and 38.0%, respectively.

The chemical composition of the main components of corn crop residues fraction I in comparison with CCR after washing with cold and hot water and representatives

Table 1 Chemical composition of the main components of plant raw materials

Plant raw material	Extraction in		RFW[a] (%)	Cellulose, (%)	Lignin, (%)	Ash, (%)
	H_2O %	NaOH %				
Corn crop residuals (CCR)	14.9 ± 0.3	40.0 ± 0.7	1.7 ± 0.2	44.5 ± 3.1	19.3 ± 0.5	3.2 ± 0.1
CCR after washing with cold water	10.5 ± 0.3	39.2 ± 0.7	1,5 ± 0.2	43.0 ± 3.1	19.7 ± 0.5	2.0 ± 0.1
CCR after washing with hot water	7.8 ± 0.2	38.6 ± 0.6	1,3 ± 0.1	42.8 ± 3.1	19.8 ± 0.6	1.7 ± 0.1
Wheat straw	10.1 ± 0.4	38.4 ± 0.8	5.2 ± 0.3	44.3 ± 3.4	18.5 ± 0.6	6.6 ± 0.2
Spruce (Smook 2003)	7.3	18.3	2.9	46.1	28.5	0,2
Poplar (Smook 2003)	2.8	22.2	2.7	51.0	21.9	0.9

[a]*RFW* resin, fats, waxes

of wheat straw, coniferous and deciduous wood is given in Table 1.

A comparative analysis of the main chemical components of plant raw materials (Table 1) shows that, in terms of its composition, CCR is close to wheat straw and differs from wood in a lower content of lignin and substances extracted with an alcohol-benzene mixture (resin, fats, and waxes), and significantly higher content of substances extracted with hot water and 1% NaOH solution, as well as a higher content of mineral substances (ash). The data in Table 1 show that sifting and washing corn residues with cold and hot water naturally reduces the content of water-soluble mineral substances in it, as well as substances extracted with hot water and alkali solution, due to which the lignin content slightly increases.

The chemical composition of the ash of the original CCR, CCR of the I fraction, and CCR after washing in cold and hot water is shown in Table 2.

As can be seen from the data in Table 2, washing corn residues with cold and hot water has approximately the same effect on the content of chemical elements in the ash and significantly reduces the content of such elements as K, Fe, P, Mg, but does not remove from the plant material Ca and Si elements, which are difficult to remove in the process of delignification of plant raw materials and provide cellulose with a high residual content of the mineral component. At the same time, sieving is an effective way to clean CCR from the remains of sand and dust (Si and Ca elements). Therefore, from an economic point of view, it is recommended to sift it from dirt and small particles before the thermochemical treatment of CCR. This chemical composition of CCR a priori indicates the need to take it into account in the processes of decalcification and delignification of this plant material to obtain cellulose suitable for chemical processing, in particular, for the extraction of corn NC.

Cooking corn cellulose

To reduce the content of extractive substances in the CCR, at the first stage, they were treated with a 5% alkali solution,

Table 2 Chemical composition of mineral substances from the fractions of the corn crop residues

Chemical elements	Initial CCR	CCR after sieving	CCR after washing with cold water	CCR after washing with hot water
12 Mg	8.042 ± 0.538	9.270 ± 0.520	6.893 ± 0.467	5.793 ± 0.437
14Si	8.038 ± 0.117	6.989 ± 0.108	13.208 ± 0.134	14.584 ± 0.141
15P	5.354 ± 0.147	5.454 ± 0.142	4.555 ± 0.145	4.126 ± 0.146
16S	3.776 ± 0.083	3.882 ± 0.084	3.614 ± 0.082	3.422 ± 0.081
19 K	13.571 ± 0.091	12.630 ± 0.084	4.758 ± 0.034	4.088 ± 0.031
20Ca	57.951 ± 0.363	57.863 ± 0.354	64.598 ± 0.357	64.485 ± 0.356
22Ti	0.302 ± 0.019	0.206 ± 0.014	0.266 ± 0.020	0.513 ± 0.024
25Mn	0.256 ± 0.008	0.207 ± 0.006	0.335 ± 0.010	0.300 ± 0.010
26Fe	2.232 ± 0.022	3.055 ± 0.025	1.491 ± 0.018	2.370 ± 0.023
29Cu	0.083 ± 0.002	0.203 ± 0.003	0.053 ± 0.002	0.042 ± 0.002
30Zn	0.277 ± 0.004	0.137 ± 0.002	0.184 ± 0.003	0.194 ± 0.003
37Rb	0.025 ± 0.001	0.020 ± 0.001	0.007 ± 0.001	0.007 ± 0.001
38Sr	0.043 ± 0.001	0.036 ± 0.001	0.030 ± 0.001	0.029 ± 0.001
39Y	0.002 ± 0.001	0.001 ± 0.001	0.003 ± 0.001	0.002 ± 0.001
40Zr	0.016 ± 0.001	0.007 ± 0.001	0.005 ± 0.001	0.010 ± 0.001

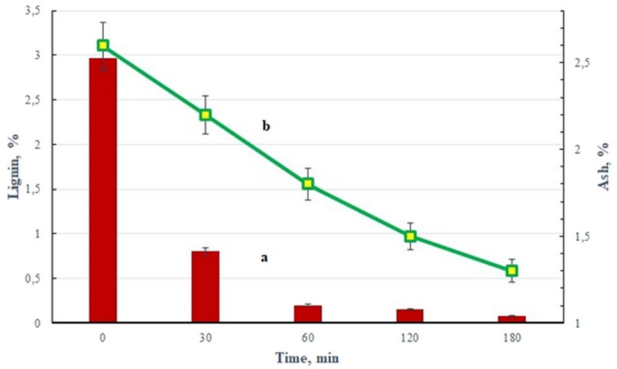

Fig. 2 Dependence of the content of lignin (**a**) and ash (**b**) in OCC on the duration of the cooking process

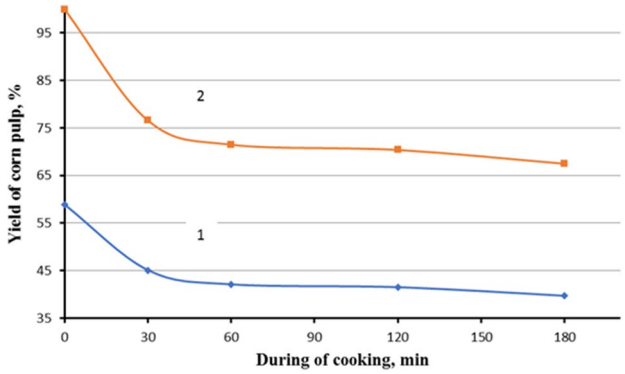

Fig. 3 Dependence of the yield of OCC on the duration of cooking: 1—relative to the raw material; 2—relative to the peracetic cooking

as a result of which corn pulp was obtained with a yield of 58.9% with a residual lignin content of 2.97% and mineral substances—2.6%, which required further delignification of corn pulp. The results of the cooking process in a peracetic acid solution for different durations are shown in Figs. 2 and 3. As can be seen from the data in Figs. 2 and 3, cooking in a solution of peracetic acid leads to a significant removal of lignin and mineral substances and a slight decrease in the yield of corn cellulose. At the same time, the high residual content of mineral substances (about 1.3%) requires an additional stage of alkaline treatment, as a result of which organosolvent cellulose (OCC) with a residual lignin content of 0.08% and 0.34% ash was obtained. OCC with such parameters is suitable for further chemical processing, in particular for the extraction of NC. The obtained OCC has better indicators than, for example, bleached spruce cellulose with a residual lignin content of 0.66% (Kumar et al. 2022) and is close to the values of organosolv cellulose obtained earlier from other representatives of non-wood plant materials—wheat straw, flax, kenaf, miscanthus, reed, hemp (Barbash and Yashchenko 2021, Barbash et al. 2022).

Structure of corn cellulosic materials

SEM analysis shows the morphological changes in the structure of corn cellulosic materials during its thermochemical processing (Fig. 4). The raw material (CCR) has an irregular porous structure (Fig. 4a). In the process of thermochemical treatment, densely located fibers of CCR are divided into separate fibers, and first partial removal occurs under the action of alkali (Fig. 4b), and then under the action of a peracetic acid solution and complete removal of lignin, which bound the fibers in the raw material, and hemicellulose and mineral substances (Fig. 4c). Under the influence of chemicals and temperature, the fibers are partially destroyed with a decrease in their transverse dimensions from 20–82 µm (for CCR, Fig. 4a) to 5–25 µm (for OCC, Fig. 4c). After acid hydrolysis, the extracted NC does not contain an amorphous part and has homogeneous nanoparticles with sizes less than tens of micrometers (Fig. 4d).

Chemical purity of corn materials

The chemical composition of the components of corn cellulose-containing materials before and after thermochemical treatments was investigated by the FTIR method (Fig. 5). Stretched peaks in the region of 3383–3485 cm^{-1} correspond to valence vibrations of O–H groups of polysaccharides with intramolecular and intermolecular hydrogen bonds (Johar et al. 2012). The spectra of all corn samples have peaks that characterize valence asymmetric (2920 cm^{-1}) and symmetric (2853 cm^{-1}) vibrations of methyl and methylene groups of cellulose. The band at 1745 cm^{-1} corresponds to the C=O valence stretching vibrations of hemicellulose carbonyl groups and lignin acetyl groups, as well as cellulose ester groups in NC (Silvério et al. 2013). The increase in the intensity of the peak at 1745 cm^{-1} for the spectrum of sample 3 (Fig. 5) is associated with the formation of carbonyl and carboxyl groups in the process of oxidation of the hydroxyl groups of cellulose under the action of peracetic acid on CPA. The absence of peaks at 1512 cm^{-1} and 1244 cm^{-1} in the spectra of cellulose and nanocellulose indicates the removal of lignin from CCR in the process of chemical and thermal treatments (Kumar et al. 2014). The bands at 1512 cm^{-1} (associated with the aromatic ring present in lignin) and 1244 cm^{-1} (associated with the aryl group in lignin) decrease sharply in the spectrum of the CPA sample. Bands in the region of 1630–1650 cm^{-1} are associated with the presence of adsorbed water, to which cellulose molecules have a strong affinity (Rosli et al. 2021).

Spectral bands observed in the range of 1420–1300 cm^{-1} in the spectra of all studied samples are associated with the scissoring motion of CH_2 in cellulose (peaks at 1426 cm^{-1}), with C–H bending (peaks at 1383 cm^{-1}), CH_2 vibrations at 1317 cm^{-1} (Kumar et al. 2014). Two peaks

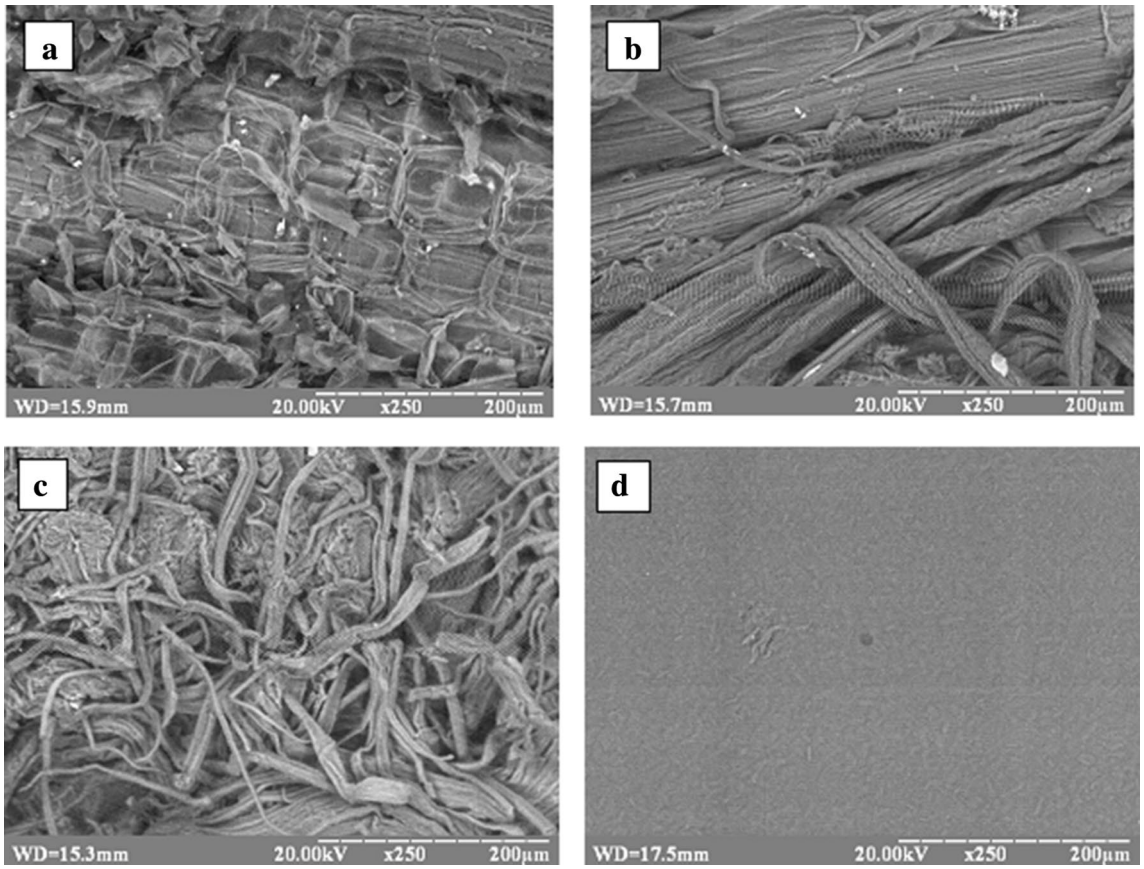

Fig. 4 SEM images: **a** CCR, **b** CPA, **c** OCC, **d** corn NC

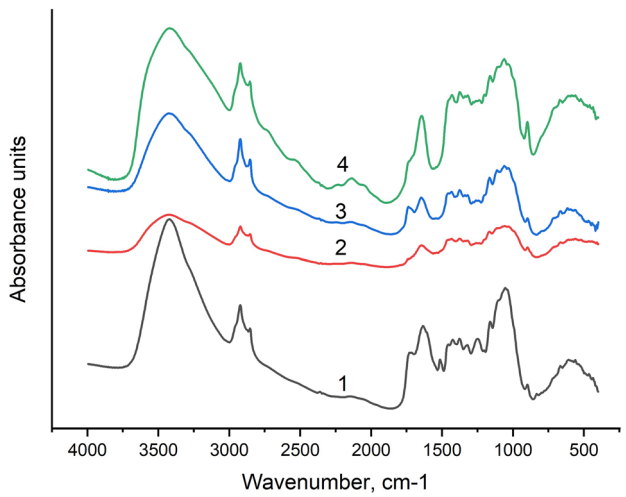

Fig. 5 FTIR spectra of samples: 1 CCR, 2 CPA, 3 OCC, 4 corn NC

at 1076 cm^{-1} and 895 cm^{-1} indicate C–O–C stretching vibration of the pyranose ring and cellulose β-glycosidic bonds (Hospodarova et al. 2018).

The growth of the peaks at 1427 cm^{-1} and 897 cm^{-1} confirm the increase in the cellulose content in the OCC and NC samples. As is known (O'Connor et al. 1958), the region of 850–1500 cm^{-1} is sensitive to the crystalline structure of cellulose material. In particular, the intensity of the spectral bands at 1420–1430 cm^{-1} and 893–897 cm^{-1} are used to determine the lateral order index (LOI) of cellulosic material. The values of the calculated LOI for the studied cellulosic corn materials are shown in Table 3. The obtained LOI values indicate a decrease in the size of the crystalline structure of corn cellulosic materials in the process of their thermochemical processing from the CCR to NC, which is confirmed by the data of other researchers (Poletto et al. 2014; Kumar et al. 2014).

XRD analysis

X-ray diffraction patterns of CCR, CPA, OCC and corn NC are shown in Fig. 6. XRD peaks in the interval 2 theta 20.7°–22.5° refer to the crystallographic plane (200) of cellulose I. Peaks in the range 13.2°–14.6° correspond to the crystallographic plane (1–10), in the range 15.4°–15.7°—crystallographic plane (110), and near

Table 3 Crystallinity characteristics of cellulosic corn materials

Corn materials	Lateral order index (LOI), 1426/897 cm^{-1}	Crystallinity index (CrI), %	Crystal size (CrS), nm
Corn crop residues (CCR)	3.000 ± 0.021	60.7 ± 0.10	3.447 ± 0.024
Corn pulp after alkaline extraction (CPA)	2.816 ± 0.019	68.3 ± 0.12	3.201 ± 0.022
Organosolv corn cellulose (OCC)	2.625 ± 0.017	72.4 ± 0.14	2.987 ± 0.018
Corn nanocellulose (NC)	1.594 ± 0.015	74.9 ± 0.16	2.636 ± 0.016

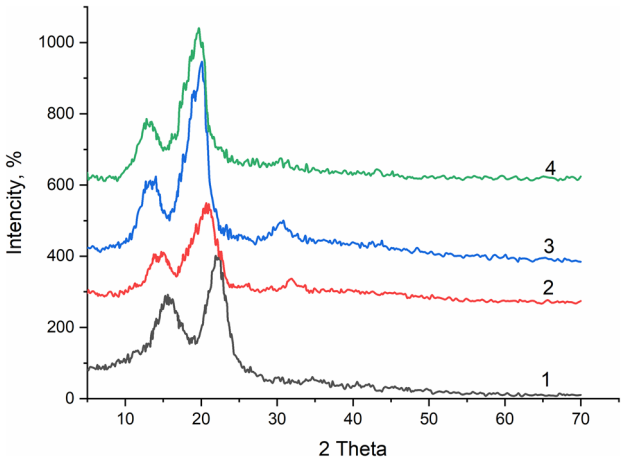

Fig. 6 X-ray diffraction patterns of: 1 CCR, 2 CPA, 3 OCC, 4 corn NC

33.2°–35°—crystallographic plane (004) of cellulose I (Ford et al. 2010). In the range 2 theta 40°–70°, additional peaks are not observed on X-ray diffractograms. The crystallinity of cellulose samples is characterized by the ratio of crystalline and amorphous parts in them and is determined in particular by the crystallinity index (CrI). CrI values calculated by Segal's method according to Eq. (1) for the tested samples are given in Table 3.

As can be seen from the data in Table 3, the CrI values of corn cellulosic materials increase in the following order: CCR-CPA-OCC—NC. The increase in the crystallinity index occurs due to the removal of extractive substances (hemicellulose and lignin) from CCR in the process of chemical and temperature action on them, which leads to an increase in the proportion of crystalline areas of cellulose. An increase in the value of CrI in the above order is also characteristic of other representatives of plant raw materials (Nuruddin et al. 2014; Sosiati et al. 2017; Sihag et al. 2022).

The apparent crystallite size (CrS) or, more precisely, the size of the coherent scattering regions in the direction normal to the reflecting plane—perpendicular to the (200) crystallographic plane, of the cellulosic materials was determined from the X-ray lines using the Scherer's formula (2). As shown in Table 3, the CrS values decrease from CCR to corn NC, which is explained by reducing the size of their crystallites in the process of sequential thermochemical processing of investigated cellulosic materials. The calculated apparent crystallite size of corn nanocellulose is in the range of values obtained by other researchers for various plants, for which CrS values range from 1.9 to 4.0 (Poletto et al. 2014; Kumar et al. 2014; Torlopov et al. 2017; Klochko et al. 2021).

Properties of corn nanocellulose

Corn NC after hydrolysis and ultrasonic treatment had the appearance of a transparent homogeneous and stable suspension (Fig. 1). The stability of the transparent gel-like suspension of NC is preserved during a long storage period at room temperature (up to a year). The nature of the stabilization of the NC colloidal suspension is explained by the presence of charged groups on its surface, which are formed during the interaction of cellulose with sulfuric acid as a result of the esterification reaction (Reising et al. 2012).

Prepared corn NC films had the following parameters: density 1.2 g/cm^3, transparency 57% at the wavelength of 600 nm, and tensile strength 43 MPa. The stress–strain curve for a corn nanocellulose film under uniaxial tension is shown in Fig. 7a. As can be seen from the data, at the initial stage of loading of the NC sample, a low strain (< 0.2%) is observed, which corresponds to the elastic zone of Young's modulus. In the strain interval of 0.2–0.4%, a "knee-like" dependence is observed for the values of tensile strength in the range of 20–32 MPa, which corresponds to the imaginary yield point, after which the region of linear high-deformation plasticity is observed. The resulting corn NC has higher tensile strength (43 MPa) and Young's Modulus (4.1 GPa) compared to paper (6 MPa and 2.7 GPa, respectively), but lower elongation values—1.07 versus 5.6% for paper (Lay et al. 2016). Numerical values of the mechanical properties of NC films can vary in a wide range depending on the raw materials, sizes, morphology, and degree of crystallinity of the fibers.

According to the data of the dynamic light scattering (DLS) method (Fig. 7b), a polydisperse distribution of particles is observed for the corn NC suspension. As shown in Fig. 7b, the intensity distribution of corn NC particles has two groups of particles: i—with peaks in the size range of

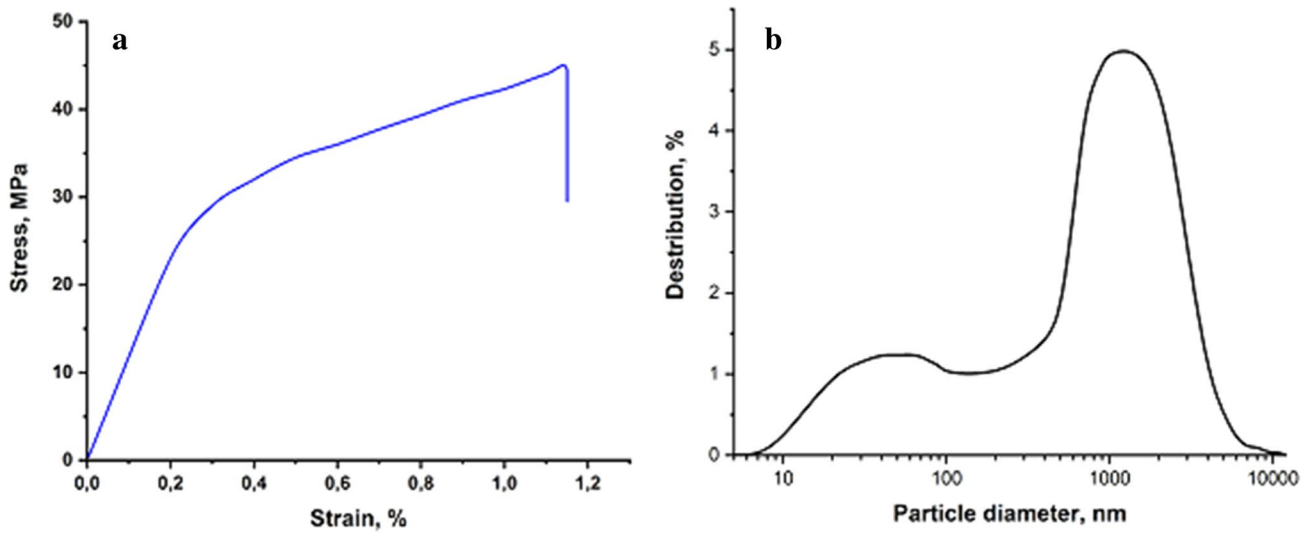

Fig. 7 The stress–strain curve for corn NC films (**a**) and particle size distribution of corn NC determined by DLS (**b**)

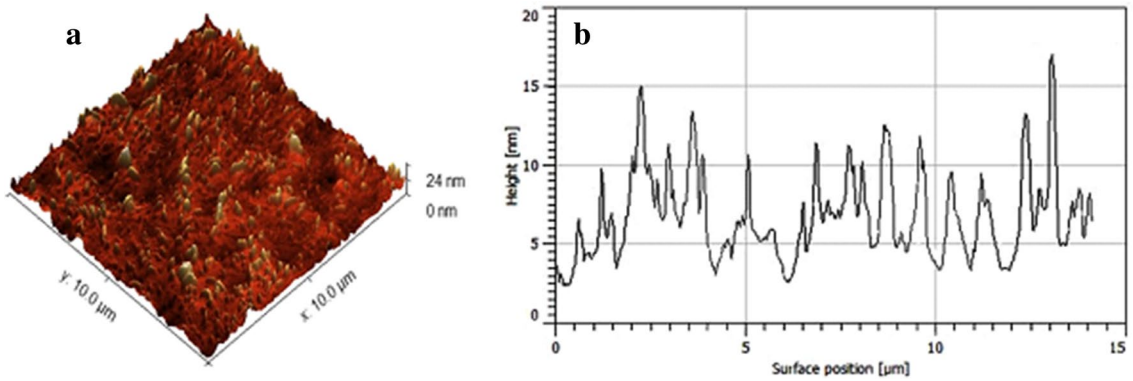

Fig. 8 AFM images of corn NC films: **a** 3D and **b** surface position

20–80 nm and ii—with peaks of particle sizes from 800 nm to 2 µm, which were interpreted as their width and length, respectively. These results indicate a high dispersion of corn NC suspension particles in size and are in good agreement with data obtained by other authors (Benini et al. 2018; Ribeiro et al. 2020; Tarres et al. 2022). The sizes of corn NC particles indicate the extraction of nanofibrillated cellulose from CCR.

The morphological and topographical structure of the obtained corn NC was analyzed using AFM (Fig. 8) and TEM (Fig. 9). In Fig. 8a shows a 3D image of the corn NC surface, which has a dust-like profile with protrusions of nanoparticles up to 24 nm. AFM image in Fig. 8b shows that the nanoparticles of corn NC have a transverse size in the range of 3–18 nm and a length of tens of micrometers. As can be seen from TEM data (Fig. 9), the obtained corn NC is nanofibrillated cellulose with a multilayer structure. Nanofibers form a fine mesh as a result of the interaction

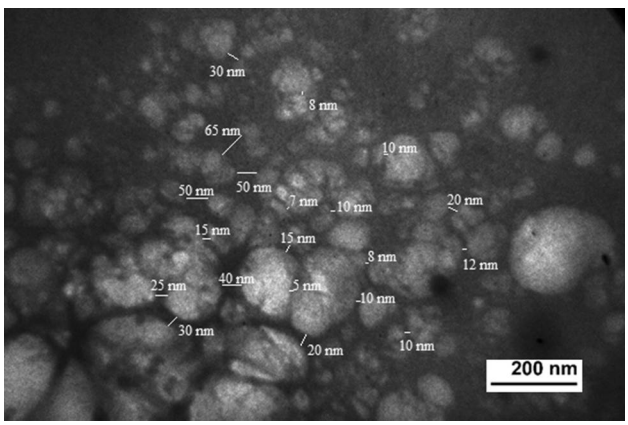

Fig. 9 TEM image of corn NC

between nanocellulose particles and have a high aspect ratio. It was experimentally established that the transverse size of individual NC nanoparticles varies from 5 to 65 nm, and their length reaches several micrometers. Similar results are observed for NC obtained by acid hydrolysis of cellulose from various representatives of non-wood plant materials (Abdul Khalil et al. 2014; Moran et al. 2008; Isogai 2020; Madivoli et al. 2020; Barbash and Yashchenko 2020, 2021, Barbash et al. 2022).

Thermal stability of CCR, CPA, OCC, and corn NC has been studied by thermogravimetric (TG) and derivative thermogravimetric (DTG) analyzes as shown in Fig. 10. Thermogravimetric curves show changes in the mass of samples during heating, and DTGs show temperature peaks at which significant weight loss occurs. As can be seen from the data in Fig. 10, the processes of thermal destruction of the studied samples can be conditionally divided into four sections: I—loss of absorbed water up to 200 °C; II—loss of bound water and degradation of cellulose and its components at temperatures from 200 to 360 °C; III—slow process of carbonization of solid residue at temperatures from 360 to 450 °C and IV—carbonization of residual products above 450 °C. For sections II and III, in which the mass reduction processes of cellulosic materials occur most dynamically, Table 4 shows such parameters of thermal degradation as the temperature of the onset of degradation (T_0), the maximum temperature of degradation (T_{max}) and the corresponding residual weight of the sample at T_{max} (RW), which were calculated from the data of the TG and DTG curves.

TG curves show that the initial temperature of mass loss for all tested samples is about 100 °C (Fig. 10a), which is associated with the evaporation of free moisture. For raw materials (CCR), thermal destruction begins at a temperature of 207.4 °C and the main part of it is destroyed in the temperature range of 270–330 °C, after which only about 30% of the mass of CCR remains. In this temperature interval, the decomposition of its least stable components occurs with the release of simple compounds—water, sulfur dioxide, carbon monoxide, and acetic acid. The second peak of CCR destruction is observed at a temperature of 410–440 °C, after which only 10% of the mass remains. At these temperatures, exothermic reactions of thermal destruction of polymers of CCR occur with the formation of gaseous and liquid products—CO_2, methanol, and acetic acid.

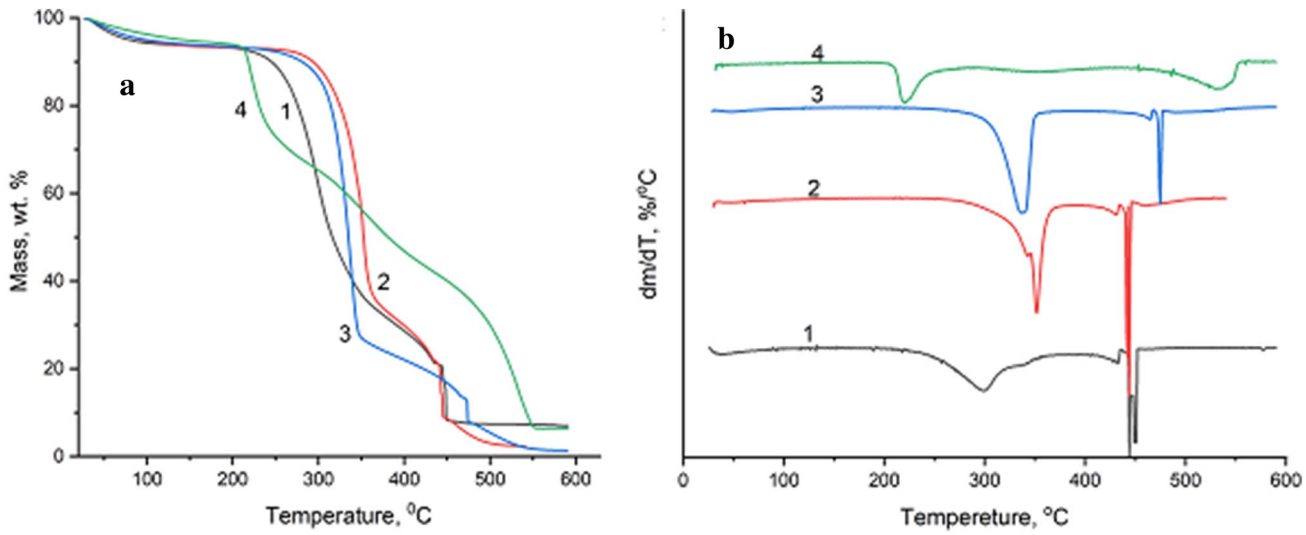

Fig. 10 TG (**a**) and DTG (**b**) curves: 1 CCR, 2 CPA, 3 OCC, 4 corn NC

Table 4 Thermal degradation parameters of the studied samples

Sample	T_0, °C	Section II		Section III		Residue (%) at temperature	
		T_{max}, °C	RW, %	T_{max}, °C	RW, %	T, °C	Residue, %
CCR	207.4	298.9	60.2	430.9	22.5	590.5	6.97
CPA	249.5	352.9	48.5	439.8	20.4	541.2	2.34
OCC	244.2	337.5	42.3	467.8	15.2	588.0	1.35
Corn	204.2	222.4	84.2				
NC		351.8	55.3	533.1	16.3	590.9	6.42

At higher temperatures (up to 600 C), charcoal remains in the residue.

The mass loss of samples (2) and (3) occurs under approximately the same conditions. In particular, the temperature at the beginning of the inflection on the TG curves for CPA and OCC are 301.7 °C and 307.2 °C, respectively. But at the end of section II, the OCC sample loses almost 20% more mass than the CPA. This is due to the fact that CPA, unlike OCC, contains some residual content of lignin and mineral substances, which are more resistant to temperature effects compared to pure cellulose.

The temperature stability of corn NC has a slightly different character (curve 4). Nanocellulose films are characterized by gradual mass loss (up to 30%) in the temperature range of 250–500 °C, which is confirmed by a smooth small peak on the differential curve (Fig. 10b). At a temperature of 500 °C, up to 30% of the mass of corn NC is preserved, while for samples CCR, CPA and OCC at this temperature only 7%, 3% and 5% of the mass remains, respectively. That is, the data of thermographic analysis indicate the formation of a dense homogeneous structure between nanocellulose particles as a result of thermochemical treatment and the action of ultrasound. The onset of the destruction of corn NC films at a lower temperature than that of plant raw materials and OCC is explained by the presence of ester sulfate groups and a larger number of free ends of NC chains (Kumar et al. 2014). Ester sulfate groups reduce the thermal stability of corn nanoparticles because they require less energy than for the destruction of the glucopyranose ring of OCC. The onset of decomposition of corn NC at lower temperatures may also indicate faster heat exchange in its samples. It was also established that the number of coal residues in the samples from corn NC is noticeably higher than in the samples of CPA and OCC (Table 4), which is confirmed by the data of other authors (Ren et al. 2022). Corn NC, like cellulose, is not a thermoplastic material, but in combination with other substances (in particular cellulose ethers and esters), it can be considered as one of the components of a composite thermoplastic material (Immonen et al. 2021). The possibilities of using NC as a component of thermoplastic material require detailed research.

Use of corn nanocellulose

The extracted corn NC is characterized by the above-mentioned properties, which are close to the parameters of nanocellulose obtained by us for various representatives of non-wood plant materials (Barbash and Yashchenko 2020, 2021, Barbash et al. 2022) and can be used as a reinforcing additive in the production of composite materials and as a basis for obtaining devices of smart flexible electronics (Sharma et al. 2019; Klochko et al. 2020, 2021; Liu et al. 2022).

In this paper, we used corn NC in the production of one of the mass types of the paper industry—cardboard for flat layers of corrugated cardboard. At the same time, the possibility of partial replacement of the chemical auxiliary substance—alkyl ketene dimer (AKD), which is produced from exhaustive energy sources and is traditionally used as a reinforcing additive in the production of cardboard with a consumption of 6 kg/t, was investigated. Table 5 shows the indicators of cardboard without and with the addition of NC and AKD at different consumptions.

As can be seen from the above data, the addition of corn NC to the fibrous composition naturally improves all cardboard indicators. The improvement of the characteristics of the cardboard, when nanocellulose is added into its composition, occurs due to the filling of voids and the formation of additional hydrogen bonds between the hydroxyl groups of the cellulose macromolecules of waste paper and nanoparticles of corn NC. It was established that the use of NC with a consumption of 5 kg/t (option 6) leads to obtaining cardboard with a value of absolute compressive strength that meets the requirements of the standard. At the same time, the value of the ring crush test was exceeded by 16.5%, the water absorption was reduced by 20%, and the consumption of environmentally harmful AKD was reduced by 50%.

Table 5 Properties of cardboard for flat layers of corrugated cardboard with and without adding of corn NC

No. of option	Consumption, kg/t		Absolute compressive resistance, KPa	Ring crush test (RCT), *N*	Water absorption $Cobb_{60}$, g/m^2
	AKD	NC			
1	–	–	274 ± 14	191 ± 10	253 ± 7.6
2	3.0	0	291 ± 15	200 ± 11	34 ± 2.4
3	1.5	0	284 ± 14	197 ± 11	42 ± 2.7
4	1.5	1.5	312 ± 16	209 ± 12	32 ± 2.3
5	1.5	3.0	338 ± 17	218 ± 13	27 ± 1.8
6	1.5	5.0	366 ± 18	233 ± 14	24 ± 1.5
7	1.5	10.0	382 ± 19	248 ± 15	21 ± 1.3
Requirements of standard			> 360	> 200	< 30

Conclusion

Corn crop residues (CCR) were used as cellulosic sources for the extraction of nanocellulose. The effect of mechanical sieving and washing of CCR in cold and hot water on the content of chemical elements in mineral substances was investigated. It has been established that pre-washing CCR with hot or cold water reduces the content of such chemical elements as K, Fe, P, Mg, but does not remove Ca and Si. Before thermochemical treatment of crushed CCR, it is recommended to sift them from sand and dust. Organosolv corn cellulose (OCC) is obtained after three stages of CCR processing: alkaline extraction, cooking in an environmentally friendly solution of peracetic acid and additional alkaline treatment to minimize the residual content of lignin and minerals. As a result of the action of a 43% solution of sulfuric acid on OCC, corn nanocellulose(NC) was obtained, which had a density of up to 1.2 g/cm^3, a tensile strength of up to 43 MPa, a transparency of up to 57%, and a crystallinity index of 74.9%, which is close to these values of nanocellulose, obtained from other representatives of non-wood plant materials. SEM data confirmed the destruction and decrease in the size of CCR fibers during their thermochemical treatment. FTIR and XRD data showed that the influence of chemicals and temperature leads to a decrease in the content of residual lignin, the lateral order index, the apparent size of crystallites and an increase in the crystallinity index in corn cellulosic materials in the following order: CCR—corn pulp after alkaline extraction, OCC—NC. DLS, AFM, and TEM data confirmed the production of corn NC, the particles of which had a transverse size of 5–65 nm and a length of up to several micrometers. On the curves of TG and DTG, the processes of thermal destruction of the studied samples are conditionally divided into four sections, for which the values of the corresponding parameters are determined. Thermographic analysis data confirm the formation of a dense homogeneous structure between the particles of corn NC as a result of thermochemical treatment and the action of ultrasound. The positive effect of the use of corn NC on the improvement of cardboard indicators and the reduction of the consumption of harmful chemical auxiliary substances is shown. Corn nanocellulose with such characteristics can be used as a reinforcing additive in the production of composite materials and as a basis for obtaining smart electronic devices, as shown in (Barbash et al. 2020, 2022; Klochko et al. 2020, 2021).

Acknowledgements The authors express their gratitude to the Ministry of Education and Science of Ukraine for financial support in the implementation of project No. 2301.

Data availability The availability of such data is complemented by links to relevant articles.

Declarations

Conflict of interest The authors declare that they have no competing interests.

References

Abdul Khalil HPS, Davoudpour Y, Islam MN, Mustapha A, Sudesh K, Dungani R, Jawaid M (2014) Production and modification of nanofibrillated cellulose using various mechanical processes: a rewiew. Carbohydr Polym 99:649–665

Alavi M (2019) Modifications of microcrystalline cellulose (MCC), nanofibrillated cellulose (NFC), and nanocrystalline cellulose (NCC) for antimicrobial and wound healing applications. E-Polymers 19:103–119

Azeredo HM, Rosa MF, Mattoso LHC (2017) Nanocellulose in bio-based food packaging applications. Ind Crops Prod 97:664–671. https://doi.org/10.1016/j.indcrop.2016.03.013

Barbash VA, Yashchenko OV (2020) Preparation and application of nanocellulose from non-wood plants to improve the quality of paper and cardboard. Appl Nanosci 10:2705–2716. https://doi.org/10.1007/s13204-019-01242-8

Barbash V, Yashchenko O (2021) Preparation, properties and use of nanocellulose from non-wood plant materials. In: Krishnamoorthy K (ed) Novel nanomaterials. IntechOpen, London. https://doi.org/10.5772/intechopen.94272

Barbash VA, Yashchenko OV, Yakymenko OS, Zakharko RM, Myshak VD (2022) Preparation of hemp nanocellulose and its application for production of paper for automatic food packaging. Cellulose. https://doi.org/10.1007/s10570-022-04773-6

Benchikh L, Merzouki A (2019) Comparative study of extraction of cellulose nanocrystals (CNC) from wood pulp. Algerian J Mat Chem 2(2):62–69

Benini KCC, Voorwald HJC, Cioffi MOC, Rezende MC, Rezende V (2018) Preparation of nanocellulose from Imperata brasiliensis grass using Taguchi method. Carbohyd Polym 192:337–346. https://doi.org/10.1016/j.carbpol.2018.03.055

Biana H, Gaoa Y, Yanga Y, Fang G, Daia H (2018) Improving cellulose nanofibrillation of waste wheat straw using the combined methods of prewashing, p-toluenesulfonic acid hydrolysis, disk grinding, and endoglucanase post-treatment. Bioresource Technol 256:321–327. https://doi.org/10.1016/j.biortech.2018.02.038

Coseri S (2009) Phthalimide-N-oxyl (PINO) radical, a powerful catalytic agent: its generation and versatility towards various organic substrates. Catal Rev Sci Eng 51(2):218–292. https://doi.org/10.1080/01614940902743841

Deepa B, Abraham E, Cordeiro N, Mozetic M, Mathew AP, Oksman K, Faria M, Thomas S, Pothan LA (2015) Utilization of various lignocellulosic biomass for the production of nanocellulose: a comparative study. Cellulose 22:1075–1090. https://doi.org/10.1007/s10570-015-0554-x

Deykun I, Halysh V, Barbash V (2018) Rapeseed straw as an alternative for pulping and papermaking. Cellulose Chem Technol 52(9–10):833–839

Du H, Liu W, Zhang M, Si C, Zhang X, Li B (2019) Cellulose nanocrystals and cellulose nanofibrils based hydrogels for biomedical applications. Carbohydr Polym 209:130–144. https://doi.org/10.1016/j.carbpol.2019.01.020

Fahmy Y, Fahmy TY, Mobarak F, El-Sakhawy M, Fadl M (2017) Agricultural residues (wastes) for manufacture of paper, board, and miscellaneous products: background overview and future prospects. Int J ChemTech Res 2(10):424–448

Ford ENJ, Mendon SK, Thames SF, Rawlins JW (2010) X-ray diffraction of cotton treated with neutralized vegetable oil-based

macromolecular crosslinkers. J Eng Fibers Fabr 5(1):10–20. https://doi.org/10.1177/155892501000500102
Gopakumar DA, Pai AR, Sisanth KS, Thomas S, Sabu KT, Grohens Y (2018) Nanocellulose: environmental and engineering applications of. Encyclopedia of polymer applications. Taylor and Francis, Boca Raton, pp 1813–1828
Hospodarova V, Singovszka E, Stevulova N (2018) Characterization of cellulosic fibers by FTIR spectroscopy for their further implementation to building materials. Am J Anal Chem 9(6):303–310. https://doi.org/10.4236/ajac.2018.96023
Hu Z, Zhai R, Li J, Zhang Y, Lin J (2017) Preparation and characterization of nanofibrillated cellulose from bamboo fiber via ultrasonication assisted by repulsive effect. Int J Polym Sci. https://doi.org/10.1155/2017/9850814
Hu M, Chen J, Yu Y, Liu Y (2022) Peroxyacetic acid pretreatment: a potentially promising strategy towards lignocellulose biorefinery. Molecules 27(19):6359. https://doi.org/10.3390/molecules27196359
Ilari A, Duca D, Boakye-Yiadom K, Gasperini T, Toscano G (2022) Carbon footprint and feedstock quality of a real biomass power plant fed with forestry and agricultural residues. Resources 11(7):1–20. https://doi.org/10.3390/resources11020007
Immonen K, Willberg-Keyriläinen P, Ropponen J, Nurmela A, Metsä-Kortelainen S, Kaukoniemi OV, Kangas H (2021) Thermoplastic cellulose-based compound for additive manufacturing. Molecules 26:1701. https://doi.org/10.3390/molecules26061701
Isogai A (2020) Emerging nanocellulose technologies: recent developments. Adv Mater 33(28):2000630. https://doi.org/10.1002/adma.202000630
Jiang Y, Liu X, Yang S, Song X, Wang S (2019) Combining organosolv pretreatment with mechanical grinding of sugarcane bagasse for the preparation of nanofibrillated cellulose in a novel green approach. BioResources 14(1):313–335
Johar N, Ahmad I, Dufresne A (2012) Extraction, preparation and characterization of cellulose fibres and nanocrystals from rice husk. Ind Crops Prod 37(1):93–99. https://doi.org/10.1016/j.indcrop.2011.12.016
Kang Y, Deng C, Chen Y, Liu X, Liang Z, Li T, Hu Q, Zhao Y (2020) Binder-free electrodes and their application for Li-ion batteries. Nanoscale Res Lett 15:112. https://doi.org/10.1186/s11671-020-03325-w
Karbalaei EMH, Talaeipour M, Bazyar B, Mirshokraei SA, Khademi Eslam H (2019) Two-step delignification of peracetic acid and alkali from sugar cane bagasse. BioRes 14(4):9994–10003
Kaur M, Sharma P, Kumari S (2017) Extraction preparation and characterization: nanocellulose. Int J Sci Res 6:1881–1886. https://doi.org/10.21275/13121701
Klochko NP, Barbash VA, Klepikova KS, Kopach VR, Tyukhov II, Yashchenko OV, Zhadan DO, Petrushenko SI, Dukarov SV, Sukhov VM, Khrypunova AL (2020) Efficient biodegradable flexible hydrophobic thermoelectric material based on biomass-derived nanocellulose film and copper iodide thin nanostructured layer. Solar Energy 212:231–240. https://doi.org/10.1016/j.solener.2020.10.081
Klochko NP, Barbash VA, Petrushenko SI, Kopach VR, Zhadan DO, Yashchenko OV, Dukarov SV, Sukhov VM, Khrypunova AL (2021) Thermoelectric textile devices with thin films of nanocellulose and copper iodide. J Mater Sci Mater Electron 32:23246–23265. https://doi.org/10.1007/s10854-021-06810-9
Kumar A, Negi YS, Choudhary V, Bhardwaj NK (2014) Characterization of cellulose nanocrystals produced by acid-hydrolysis from sugarcane bagasse as agro-waste. J Mater Phys Chem 2(1):1–8
Kumar V, Pathak P, Bhardwaj NK (2020) Waste paper: an underutilized but promising source for nanocellulose mining. Waste Manag 102:281–303. https://doi.org/10.1016/j.wasman.2019.10.041
Kumar P, Miller K, Kermanshahi A, Brar SK, Beims RF, Xu CC (2022) Nanocrystalline cellulose derived from spruce wood: Influence of process parameters. Int J Biol Macromol 221(30):426–434. https://doi.org/10.1016/j.ijbiomac.2022.09.017
Lay M, Méndez JA, Pèlach MA, Vilaseca F (2016) Combined effect of carbon nanotubes and polypyrrole on the electrical properties of cellulose-nanopaper. Cellulose. https://doi.org/10.1007/s10570-016-1060-5
Lee KY, Blaker JJ, Heng JY, Murakami R, Bismarck A (2014) pH-triggered phase inversion and separation of hydrophobised bacterial cellulose stabilised Pickering emulsions. React Funct Polym 85:208–213. https://doi.org/10.1016/j.reactfunctpolym.2014.09.016
Liu D, Gao Y, Song Y, Zhu H, Zhang L, Xie Y, Shi H, Shi Z, Yang Q, Xiong C (2022) Highly sensitive multifunctional electronic skin based on nanocellulose/mxene composite films with good electromagnetic shielding biocompatible antibacterial properties. Biomacromol 23(1):182–195. https://doi.org/10.1021/acs.biomac.1c01203
Madivoli ES, Kareru PG, Gachanja AN, Mugo SM, Sujee DM, Fromm KM (2020) Isolation of cellulose nanofibers from oryzasativa residues via TEMPO mediated oxidation. J Nat Fibers. https://doi.org/10.1080/15440478.2020.1764454
Moran JI, Alvarez VA, Cyras VP, Vázquez A (2008) Extraction of cellulose and preparation of nanocellulose from sisal fibers. Cellulose 15(1):149–159. https://doi.org/10.1007/s10570-007-9145-9
Nagarajan KJ, Ramanujam NR, Sanjay MR, Siengchin S, Surya Rajan B, Sathick Basha K, Madhu P, Raghav GR (2021) A comprehensive review on cellulose nanocrystals and cellulose nanofibers: pretreatment, preparation, and characterization. Polym Compos 42(4):1588–1630. https://doi.org/10.1002/pc.25929
Nehra P, Chauhan RP (2021) Eco-friendly nanocellulose and its biomedical applications: current status and future prospect. J Biomater Sci Polym Ed 32(1):112–149. https://doi.org/10.1080/09205063.2020.1817706
Nuruddin M, Hosur M, Triggs E, Jeelani S (2014) Comparative study of properties of cellulose nanofibers from wheat straw obtained by chemical and chemi-mechanical treatments. In: Proceedings of the ASME 2014 international mechanical engineering congress & exposition, November 14–20, Montreal, Canada, V014T11A042, ASME. https://doi.org/10.1115/IMECE2014-36174
O'Connor RT, DuPre EF, Mitcham D (1958) Application of infrared absorption spectroscopy to investigations of cotton and modified cottons. Part 1: physical and crystalline modifications and oxidation. Textile Res J 28:382–392
Poletto M, Ornaghi Júnior HL, Zattera AJ (2014) Native cellulose: structure, characterization and thermal properties. Materials 7:6105–6119. https://doi.org/10.3390/ma7096105
Randhawa A, Dutta SD, Ganguly K, Patil TV, Patel DK, Lim KT (2022) A review of properties of nanocellulose, its synthesis, and potential in biomedical applications. Appl Sci 12:7090. https://doi.org/10.3390/app12147090
Reising AB, Moon RJ, Youngblood JP (2012) Effect of particle alignment on mechanical properties of neat cellulose nanocrystal films. J Sci Technol Forest Products Processes 2(6):32–41
Ren S, Sun X, Lei T, Wu Q (2014) The effect of chemical and high-pressure homogenization treatment conditions on the morphology of cellulose nanoparticles. J Nanomater. https://doi.org/10.1155/2014/582913
Ren RW, Chen XQ, Shen WH (2022) Preparation and separation of pure spherical cellulose nanocrystals from microcrystalline cellulose by complex enzymatic hydrolysis. Int J Biol Macromol 202:1–10
Reshmy R, Philip E, Paul S et al (2020) Nanocellulose-based products for sustainable applications: recent trends and

possibilities. Rev Environ Sci Biotechnol. https://doi.org/10.1007/s11157-020-09551-z
Ribeiro RSA, Bojorge N, Pereira N (2020) Statistical analysis of the crystallinity index of nanocellulose produced from Kraft pulp via controlled enzymatic hydrolysis. Biotechnol Appl Biochem. https://doi.org/10.1002/bab.1873
Rosli NA, Ishak WHW, Ahmad I (2021) Eco-friendly high-density polyethylene/amorphous cellulose composites: environmental and functional value. J Cleaner Prod 290:125886–131259
Segal LC, Creely JJ, Martin AEJ, Conrad CM (1959) An empirical method for estimating the degree of crystallinity of native cellulose using the x-ray diffractometer. Text Res J 29(10):786–794. https://doi.org/10.1177/004051755902901003
Sharma A, Thakur M, Bhattacharya M, Mandal T, Goswamia S (2019) Commercial application of cellulose nano-composites—a review. Biotechnol Rep. https://doi.org/10.1016/j.btre.2019.e00316
Sihag S, Sheetal, Yadav M, Pal J (2022) Extraction and characterization of nanocellulose from wheat straw. J Water Environ Nanotechnol 7(3):317–331
Silvério HA, Neto WPF, Dantas NO, Pasquini D (2013) Extraction and characterization of cellulose nanocrystals from corncob for application as reinforcing agent in nanocomposites. Ind Crops Prod 44:427–436. https://doi.org/10.1016/j.indcrop.2012.10.014
Smith CW, Javier B, Runge ECA (2004) Corn: origin, history, technology, and production. Wiley, p 976 (**ISBN 978-0-471-41184-0**)
Smook GA (2003) Handbook for pulp and paper technologists, 3rd edn. Angus Wilde Publications, Inc, p 425
Sosiati H, Wijayanti D, Triyana K, Kamiel B (2017) Morphology and crystallinity of sisal nanocellulose after sonication AIP Conference Proceedings 1877, 030003. https://doi.org/10.1063/1.4999859
Su C, Hirth K, Liu Z, Cao Y, Zhu JY (2021) Maleic acid hydrotropic fractionation of wheat straw to facilitate value-added multi-product biorefinery at atmospheric pressure. GCB Bioenergy. https://doi.org/10.1111/gcbb.12866
TAPPI Test Methods, 2002-2003 (2002) Tappi Press, Atlanta, Ga., 1219 p
Sun B, Zhang M, Hou Q, Liu R, Wu T, Si C (2016) Further characterization of cellulose nanocrystal (CNC) preparation from sulfuric acid hydrolysis of cotton fibers. Cellulose 23(1):439–450. https://doi.org/10.1007/s10570-015-0803-z
Tarres Q, Aguado R, Zoppe JO, Mutjé P, Fiol N, Delgado-Aguilar M (2022) Dynamic light scattering plus scanning electron microscopy: usefulness and limitations of a simplified estimation of nanocellulose dimensions. Nanomaterials 12:4288. https://doi.org/10.3390/nano12234288
Torlopov MA, Mikhaylov VI, Udoratina EV, Aleshina LA, Prusskii AI, Tsvetkov NV, Krivoshapkin PV (2017) Cellulose nanocrystals with different length-to-diameter ratios extracted from various plants using novel system acetic acid/phosphotungstic acid/octanol-1. Cellulose 25(2):1031–1046. https://doi.org/10.1007/s10570-017-1624-z
Tu WC, Weigand L, Hummel M et al (2020) Characterisation of cellulose pulps isolated from Miscanthus using a low-cost acidic ionic liquid. Cellulose 27:4745–4761. https://doi.org/10.1007/s10570-020-03073-1